Journal of Membrane Science 685 (2023) 121904

Contents lists available at ScienceDirect

Journal of Membrane Science

journal homepage: www.elsevier.com/locate/memsci

Analytical treatment of ion-exchange permselectivity and transport number measurements for high accuracy

Simon B.B. Solberg [a], Pauline Zimmermann [a], Øivind Wilhelmsen [b], Robert Bock [c], Odne S. Burheim [a,*]

[a] Department of Energy and Process Engineering, Norwegian University of Science and Technology, NO-7491 Trondheim, Norway
[b] Department of Chemistry, Norwegian University of Science and Technology, NO-7491 Trondheim, Norway
[c] Federal Institute for Materials Research and Testing (BAM), 12205 Berlin, Germany

ARTICLE INFO

Keywords:
Ion-exchange membranes
Electrodialysis
Non-equilibrium thermodynamics
Electroosmosis
Transport number

ABSTRACT

We analyse electromotive force measurements of concentration cells using non-equilibrium thermodynamics, and determine the transference coefficients of ion-exchange membranes in aqueous KCl solutions. By taking advantage of the analytical expression for the permselectivity, we extract transport coefficients with high accuracy. The transport number of K^+ and the transference coefficient of water in the Selemion CMVN cation-exchange membrane are found to be $100t_{K^+} = 99.59 \pm 0.56$ and $t_w = 3.69 \pm 0.40$ respectively, while for the Selemion AMVN anion-exchange membrane they are $100t_{Cl^-} = 100.21 \pm 0.37$ and $t_w = -3.75 \pm 0.27$. These results suggest that the membranes are perfectly selective to the target ion, and that each ion carries 3-4 water molecules through the membrane, which reduces the membrane permselectivity. In these concentration cells, the electrical potential contribution of the membrane alone was more easily isolated with bare Ag/AgCl electrodes without reference solutions and liquid junction plugs. Additionally, we find a large contribution to the measured concentration cell voltage from concentration gradients across the porous plug of the reference electrode, which cannot be explained by Henderson's equation alone. For most of the concentration range, the transport number of the porous plug is determined to be $100t_{K^+} = 49.43 \pm 0.78$ with negligible water transport, similar to literature values for bulk electrolyte. In dilute electrolyte solutions with concentrations below 0.1 mol kg^{-1}, the plug shows anomalous behaviour consistent with an increase in K^+ selectivity and water co-transport.

1. Introduction

Ion-exchange membranes are interesting porous materials with a wide range of applications, due to their properties which allow for selective transport of ions in aqueous solutions. Electrodialysis and reverse electrodialysis are typical examples of applications, where the former is more widespread in the industry [1]. Important applications of electrodialysis include chemical and food production, waste water treatment and desalination [2,3]. Reverse electrodialysis for electricity production has seen limited industrial use [4], but novel closed loop concepts for chemical production are gaining interest [5–8]. However, the membrane performance is a vital factor for the efficacy of these applications.

For the electromembrane processes, organic polymer membranes with dispersed fixed charge groups, such as sulfonic acid or trimethylammonium, are common [9,10]. The transport is driven by a concentration gradient and/or an electric field [11]. Material properties such as the structure of pores, the charge density and hydrophobicity are important factors that influence the mobility of ions in the membrane phase [9]. Due to the hydrated state of the dissolved ionic species, the membrane's ability to repel water molecules may promote selectivity of one ionic species over another more hydrated species. The electrical resistance may, however, increase when the selectivity increases [12]. Therefore, it is of interest to know the number of water molecules carried by each ionic species inside the membrane phase. The transference coefficient of water is a relevant variable in this regard, since it describes the net transport of water by the electric current [11].

The co-transport of water, often referred to as electroosmosis, has been investigated in detail for perfluorinated Nafion membranes [2,3,13–21]. Water transference coefficients in the literature have typically been measured by streaming potential measurements, by which water transference coefficients in Nafion 115 with binary water and chloride salt solutions have been determined to be ≈2.6, ≈5 and ≈15 for H^+,

* Corresponding author.
E-mail address: odne.s.burheim@ntnu.no (O.S. Burheim).

https://doi.org/10.1016/j.memsci.2023.121904
Received 27 April 2023; Received in revised form 21 June 2023; Accepted 30 June 2023
Available online 7 July 2023

K^+ and Mg^{2+}, respectively [13]. The framework of non-equilibrium thermodynamics was used in this context, and is generally a useful tool for the description of transport phenomena in membranes [11].

Electromotive force measurements of concentration cells with an ion-exchange membrane can also be used to determine the membrane transference coefficients [22–24]. For such measurements, it is commonplace to use commercial reference electrodes with a filling solution that is separated from the testing solution by a porous ceramic plug. The concentration gradient that arises across these liquid junctions has often been neglected in the electromembrane literature, even though it has been shown to add a substantial electrical potential contribution to the measured voltage of the concentration cell [11,25,26]. The liquid junction potential is often estimated by the use of Henderson's equation, which has been shown to describe a portion of the total electric potential difference across a junction in a concentration cell with two identical electrodes. In a formation cell with two distinct electrode reactions, the total electric potential difference across the junction is adequately described by Henderson's equation, typically resulting in a small voltage contribution [11]. In a concentration cell, however, the term described by the Henderson's equation is only one of several contributions to the total electrical potential difference. In this work, we will clarify the role of junction and porous ceramic plug in the description of concentration cells by dedicated measurements and theoretical analysis.

Another goal of this work is to clarify the role of transport numbers and coefficients in the description of the ion-exchange membrane's permselectivity. In particular, we seek to unravel how the permselectivity depends on the chemical potential differences across the membrane in a concentration cell. Previous works have extracted transference coefficients by use of methods that assume small concentration differences across the membrane [22]. We alleviate this assumption for binary electrolytes by using an analytical form of the equation for the membrane permselectivity, which identifies transport coefficients with a high accuracy. Moreover, we present the first measurements of transport coefficients of water and ions in KCl.

2. Non-equilibrium thermodynamics

The transport phenomena taking place in an ion-exchange membrane used in a concentration cell can be described by non-equilibrium thermodynamics. In an isothermal binary mixture of KCl dissolved in water, the coupled steady state transport of water and ionic species across an ion-exchange membrane, wetted by aqueous solutions on either side, can be described by three flux equations [11]:

$$\begin{bmatrix} J_{K+} \\ J_{Cl-} \\ J_w \end{bmatrix} = -\frac{1}{T}\begin{bmatrix} L_{++} & L_{+-} & L_{+w} \\ L_{-+} & L_{--} & L_{-w} \\ L_{w+} & L_{w-} & L_{ww} \end{bmatrix}\begin{bmatrix} \nabla\tilde{\mu}_{K+} \\ \nabla\tilde{\mu}_{Cl-} \\ \nabla\mu_w \end{bmatrix} \tag{1}$$

where J_{K+}, J_{Cl-}, and J_w are the fluxes of K^+, Cl^- and water, respectively. The membrane in mechanical equilibrium is taken as the frame of reference. The ionic species and water fluxes arise due to a linear combination of phenomenological coefficients, L_{ij}, and the driving forces for transport. Here, the subscripts "+ ", "-" and "w" denote cations, anions and water, respectively, and ∇ is the spatial gradient operator. We consider the aqueous solutions to have uniform composition, such that concentration gradients are confined to the interior of the membrane or liquid junction. The diagonal elements of the coefficient matrix are the main coefficients for component transport, and the off-diagonal elements describe the magnitude of the coupling between fluxes, subject to the Onsager relations, $L_{ij} = L_{ji}$ [11]. The gradient of the chemical potential of water, $\nabla\mu_w$ is the main driving force for water transport. For an ionic species, k, the gradient of the *electrochemical potential*, $\nabla\tilde{\mu}_k$, mainly drives the transport. Guggenheim defined the electrochemical potentials [27], which for monovalent ions are:

$$\begin{aligned} \tilde{\mu}_+ &= \mu_+ + F\psi \\ \tilde{\mu}_- &= \mu_- - F\psi \end{aligned} \tag{2}$$

where μ_k is the chemical potential of the ionic species k, and F is the Faraday constant. The electrostatic potential, ψ, is *not* the measurable electric potential, ϕ, of the cell, but the two are related through [11]:

$$\phi = \psi - \frac{\mu_{Cl-}}{F} \tag{3}$$

provided that we have Cl^- reversible Ag/AgCl electrodes in an aqueous solution of KCl. This relation emerges due to the charge carrier changing at the electrode, from electrons in the solid phase, to aqueous ions in the liquid phase [11,27,28].

Let us only consider the fluxes in the x-direction perpendicular to the membrane. By using Eqs. (2)–(3), the flux equations in terms of measurable state variables become:

$$\begin{bmatrix} J_{K+} \\ J_{Cl-} \\ J_w \end{bmatrix} = -\frac{1}{T}\begin{bmatrix} L_{++} & F(L_{++}-L_{+-}) & L_{+w} \\ L_{-+} & F(L_{-+}-L_{--}) & L_{-w} \\ L_{w+} & F(L_{w+}-L_{w-}) & L_{ww} \end{bmatrix}\begin{bmatrix} \partial_x\mu_s \\ \partial_x\phi \\ \partial_x\mu_w \end{bmatrix} \tag{4}$$

where we used $\mu_s = \mu_{K+} + \mu_{Cl-}$, and ∂_x denotes gradients in the x-direction. The subscript s denotes the neutral salt, KCl. A consequence of the converse electrode reactions is that the net transport of KCl in the aqueous phase is defined by the K^+ flux i.e., $J_s = J_{K+}$. Due to the divergence of Cl^- at both electrodes, the concentration of KCl in the aqueous solutions is everywhere defined by the concentration of K^+. Furthermore, the current density in the aqueous phase must be due to the migration of ionic species i.e., $j = F(J_{K+} - J_{Cl-})$. These substitutions yield:

$$\begin{bmatrix} J_s \\ j \\ J_w \end{bmatrix} = -\frac{1}{T}\begin{bmatrix} L_{ss} & L_{s\phi} & L_{sw} \\ L_{\phi s} & L_{\phi\phi} & L_{\phi w} \\ L_{ws} & L_{w\phi} & L_{ww} \end{bmatrix}\begin{bmatrix} \partial_x\mu_s \\ \partial_x\phi \\ \partial_x\mu_w \end{bmatrix} \tag{5}$$

where we contracted the coefficients as: $L_{ss} = L_{++}$, $L_{s\phi} = L_{\phi s} = F(L_{++} - L_{+-})$, $L_{\phi\phi} = F^2(L_{++} - 2L_{-+} + L_{--})$, and $L_{w\phi} = L_{\phi w} = F(L_{+w} - L_{-w})$.

Only the expression for the current density is required for the treatment of electromotive force measurements across membranes. We may rearrange this equation with respect to the measurable electric potential gradient, and introduce the following parameters:

$$t_s = t_{K+} = F\left(\frac{J_s}{j}\right)_{\mathrm{d}\mu=0} = F\frac{L_{\phi s}}{L_{\phi\phi}} \tag{6}$$

$$t_w = F\left(\frac{J_w}{j}\right)_{\mathrm{d}\mu=0} = F\frac{L_{\phi w}}{L_{\phi\phi}} = F^2\frac{(L_{w+} - L_{w-})}{L_{\phi\phi}} \tag{7}$$

$$\kappa = -\left(\frac{j}{\partial_x\phi}\right)_{\mathrm{d}\mu=0} = \frac{L_{\phi\phi}}{T} \tag{8}$$

where κ is the electric conductivity, t_{K+} is the transport number of $K+$, and t_s and t_w are the transference coefficients of KCl and water, respectively. The subscript $\mathrm{d}\mu = 0$ refers to the condition with uniform composition, and constant temperature and pressure. This condition signifies that the transference coefficients describe the part of the flux attributed to migration, but they may still be determined even if a concentration gradient is present [23]. The ionic transport numbers are the fractions of the electric current carried by that ion, and the transference coefficients of the neutral salt and of water describe the movement of moles of salt and water per Coulomb of charge passing in the external circuit. Since the current density through the aqueous solutions is solely due to the migration of ions, the ionic transport numbers are related by: $t_{K+} + t_{Cl-} = 1$. Furthermore, the signs of the coefficients in the numerator of the right hand side of Eq. (7) show that cations and anions carry their hydration shells in opposite directions during migration. The water transference coefficient is therefore a function of the ionic transport numbers [11]. With the aid of the Onsager reciprocal relations, the measurable electric potential can finally be expressed in terms of the current density as:

$$\partial_x\phi = -\frac{t_{K+}}{F}\partial_x\mu_s - \frac{t_w}{F}\partial_x\mu_w - \frac{j}{\kappa} \tag{9}$$

2.1. Permselectivity

Assuming constant transference coefficients in the liquid junction, Eq. (9) may readily be integrated across the liquid junction. This assumption may be justified *a priori* based on the weak concentration dependency of the K^+ transport number in the aqueous phase observed by MacInnes and Dole [29]. It is convenient to relate the chemical potentials to more accessible variables, such as the salt molality, m_s. In the case of a single binary salt dissolved in water, the isothermal chemical potential gradients across the liquid junction may be expressed as [30]:

$$\Delta\mu_s = RT\Delta \ln a_s = \nu RT\Delta \ln\left(Qm_s\gamma_\pm\right) \tag{10}$$

$$\Delta\mu_w = RT\Delta \ln a_w = -\nu RT M_w \Delta(m_s\varphi) \tag{11}$$

where the definition of the osmotic coefficient, φ, is applied in the last equality of Eq. (11). The factor $Q = (\nu_+^{\nu_+}\nu_-^{\nu_-})^{(1/\nu)}$, where ν_+, ν_- and $\nu = \nu_+ + \nu_-$ are the stoichiometric factors in the dissolution reaction of the cation, anion and the neutral salt, respectively. For a binary monovalent salt like KCl, the factor Q is unity, and the stoichiometric factor of the neutral salt is two [30]. Lastly, M_w is the molecular weight of water, R is the universal gas constant, T is the absolute temperature, $\gamma_\pm$ is the salt activity coefficient, and a_k is the activity of component k. The activity and osmotic coefficients of aqueous KCl has been measured by a multitude of researchers using various experimental methods [31–36]. Reliable thermodynamic data and the procedure for determining the temperature correction of the activity coefficient to the experimental temperature are summarised in Appendix B.

Several ways to express the membrane permselectivity have been proposed in the literature [10]. However, the ratio of the measured electric potential of the cell to the ideal potential is the most useful one for the determination of the water transference coefficient. We express the permselectivity, α, as:

$$\alpha = F\left(\frac{\Delta\phi}{-\Delta\mu_s}\right)_{j=0} = t_{K+} + t_w\frac{\Delta\mu_w}{\Delta\mu_s} = t_{K+} - t_w M_w\frac{\Delta(m_s\varphi)}{\Delta \ln(m_s\gamma_\pm)} \tag{12}$$

Assuming that the transference coefficients remain constant, we therefore expect α to be a linear function of $\Delta\mu_w/\Delta\mu_s$ with a slope of t_w and an axis intercept at t_{K+}.

3. Statistical treatment

Two different regression models are investigated to gauge whether the water transport has a statistically significant influence on the measured voltage. The first model disregards electroosmotic transport:

$$\Delta\phi = t_{K+}\frac{\Delta\mu_s}{F} \tag{13}$$

where the measured electric potential is plotted as a function of the ideal electric potential, which yields the transport number as the regression slope. Eq. (12) was adopted as the second model, where permselectivity is defined as a function of $\Delta\mu_w/\Delta\mu_s$. These regression models are then compared using a Lack-of-Fit test. Such a test extracts the portion of the residual sum of squares that is associated with the replication of the measurements, which is then subtracted from the residual sum of squares, giving an estimate of the suitability of the model [37]. If the model adequately describes the results, the test statistic given by:

$$F_{\mathrm{LOF}} = \frac{\sum_{i=1}^{m}\sum_{j=1}^{n_i}(y_{ij}-\bar{y}_i)^2/(m-p)}{\sum_{i=1}^{m}\sum_{j=1}^{n_i}\left[(y_{ij}-\bar{y}_i)^2-(y_{ij}-\hat{y}_i)^2\right]/(n-m)} \tag{14}$$

follows a Fisher distribution. Here, y_{ij} are all measured values (replicates) and $\bar{y}_i$ is the mean of the measured values at a specific set of experimental conditions, i. Furthermore, the number of differing experimental conditions is denoted by m, p denotes the number of model parameters, n is the total number of measurement points, and $\hat{y}_i$ is the model prediction at the experimental conditions, i. The test statistic is compared to a 95% confidence level critical value for the Fisher distribution denoted by $F_{0.95,(m-p),(n-m)}$. A test statistic lower than this critical value indicates that all significant trends in the data set have been modelled by the regression.

4. Experimental method

Aqueous mixtures of various concentrations of KCl (for analysis EMSURE, supplied by Merck) were prepared using de-ionised water with a conductivity of 5.5 μS m^{-1}. The Selemion CMVN cation-exchange membranes and the Selemion AMVN anion-exchange membranes were delivered by AGC Engineering Co., Ltd. in Na+ and Cl^- forms, respectively. The membranes were stored in KCl mixtures of 0.1 mol kg^{-1}. For the first week, the storage solutions were refreshed every day to facilitate the conversion of the CEM into the K^+ form. During the subsequent four weeks, the solutions were refreshed once every week.

Two silver rods (≥99.95% Ag, 5 mm diameter, supplied by Thermo Scientific) were cut into a suitable length and polished. A 0.1 mol L^{-1} solution of HCl (1 mol L^{-1} TitriPUR, supplied by Merck) was prepared by dilution with de-ionised water. Immersed in HCl, the silver rods were electroplated with AgCl by passing 1 mA with Pt as the counter electrode for 5 h. A Gamry Interface 5000E potentiostat was used for voltage logging (with a stated standard deviation in mV of $1.96\sigma = 1 + 0.2\% \times \Delta\phi$) and electroplating. Experiments were conducted under isothermal conditions at 21.5 ± 0.5 °C. The Ag/AgCl rod electrodes were stored short-circuited in a 0.1 mol kg^{-1} KCl solution when not in use. If the average open circuit bias potential between the electrodes over 300 s was more than 1 mV and increasing, the Ag/AgCl electrodes were polished and a new AgCl layer deposited.

Using the rod electrodes, the membrane potential was measured in the cell described by:

(Cell 1)

$$Ag \mid AgCl \mid KCl\ (m_1)\ |\mathbf{M}|\ KCl\ (m_2) \mid AgCl \mid Ag$$

where |M| denotes the ion-exchange membrane, while m_1 and m_2 are the salt molalities at each side of the membrane. The salt mixtures were rigorously stirred by magnetic stirrers to prevent contributions from concentration polarisation. The mixtures were not circulated, as the voltage reduction over the course of the experiment due to diffusion was unobservable. Each half-cell compartment was 300 mL, and the exposed membrane area was 7.10 cm^2. The cells described by Cell 1 and Cell 2 are illustrated in Fig. 1. The electric potential of the cell was taken as the average voltage over a stable period of at least 600 s. Measurements with rod electrodes in saturated KCl were taken as the average over only the first 300 s, due to the AgCl layer instability resulting in a voltage drift over longer periods of time [38]. Electrode bias for the silver rods were measured in 0.1 mol kg^{-1} KCl after each membrane experiment.

Two Ag/AgCl reference electrodes (B 2820+, supplied by SI Analytics) with ceramic diaphragms and saturated KCl filling solutions were kept short-circuited in saturated KCl when not in use. The reference electrodes were used to measure the cell:

(Cell 2)

$$Ag/AgCl \mid KCl\ (\text{sat.}) \parallel KCl\ (m_1)\ |\mathbf{M}|\ KCl\ (m_2) \parallel KCl\ (\text{sat.}) \mid AgCl/Ag$$

where || denotes the porous ceramic junction, and the reference electrode bias was measured in saturated KCl. To investigate the junction contribution, the cell denoted by:

(Cell 3)

$$Ag \mid AgCl \mid KCl\ (\text{sat.}) \parallel KCl\ (m_1) \mid AgCl \mid Ag$$

was also studied. The bias potential between the reference electrode and the rod electrode was measured in saturated KCl after the cell

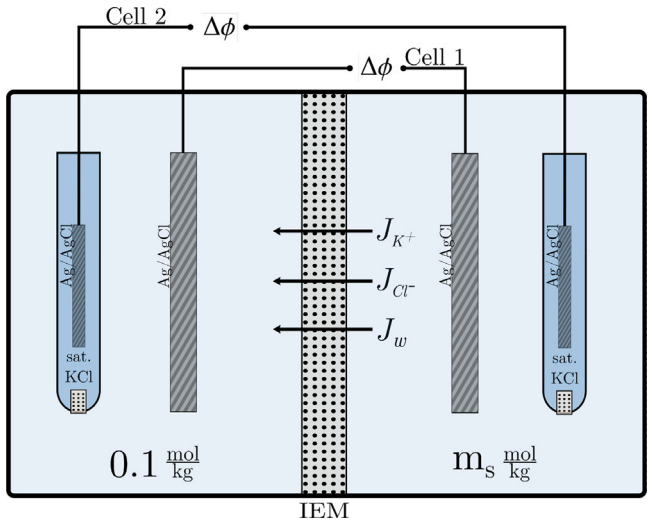

Fig. 1. Sketch of the concentration cell used in Cell 1 and Cell 2 showing local fluxes of cations, J_{K+}, anions, J_{Cl-}, and water, J_w, through the ion-exchange membrane (IEM). The right-hand side compartment's salt concentration, m_s, is varied between 0.5 mol kg^{-1} and saturated KCl.

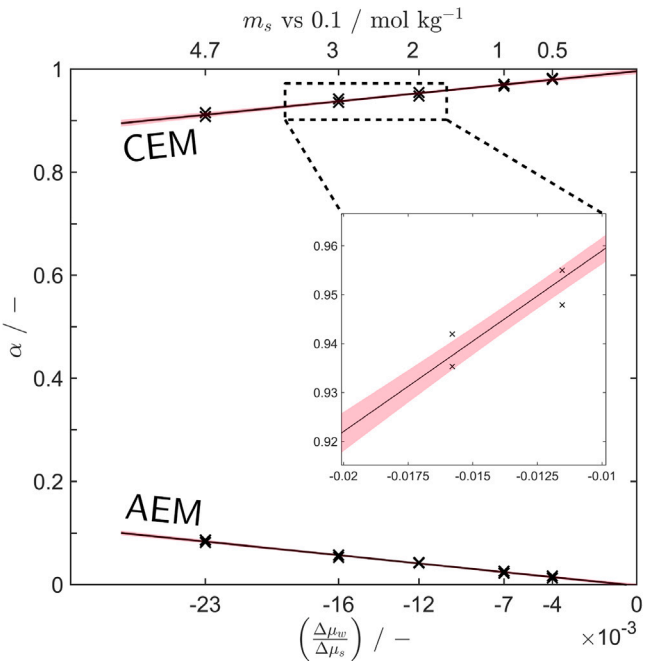

Fig. 2. Permselectivity, α, as function of the ratio of chemical potential gradients of water and salt, $\Delta\mu_w/\Delta\mu_s$, in the cell with rod electrodes. One compartment contained 0.1 mol kg^{-1} of KCl, and the top axis shows the molality of the other compartment. Measurements for the cation and anion-exchange membranes (CEM and AEM respectively) are shown as crosses, ordinary least squares regressions are shown as solid lines, and the 95% confidence interval of the regression is illustrated by the red filling. (For interpretation of the references to colour in this figure legend, the reader is referred to the web version of this article.)

measurement. All bias potentials were subtracted from the measured cell voltages, and the cell voltages were always measured from the low to the high concentration side, ensuring the same voltage sign. Measurements involving reference electrodes were maintained for at least 1800 s, but particularly in concentrations below 0.1 mol kg^{-1} periods of above 3600 s were required for voltage stabilisation.

5. Results and discussion

5.1. Measurements with Ag /AgCl Rods

The permselectivity of the Selemion CMVN and AMVN membranes, calculated as the measured electric potential divided by the ideal potential, is shown in Fig. 2 for the cell using bare Ag/AgCl rod electrodes. In this figure, the depicted ordinary least square regressions are based on Eq. (12). The transference coefficients of KCl and water are found as the regression intercept and slope, respectively. These particular ion-exchange membranes were chosen to represent a typical membrane for (reverse) electrodialysis. Due to the choice of Cl-reversible electrodes, we have the relation $t_{KCl} = t_{K+}$. From examining the mass balance of the system, we infer that only the migration of K^+ through the membrane leads to movement of neutral KCl. All measured cell voltages, with electrode bias subtracted, are shown in Appendix A. The permselectivity behaviour of the CEM is well described by the linear regression with intercept $100t_{K+} = 99.59 \pm 0.56$ and the slope $t_w = 3.69 \pm 0.40$. The confidence interval of the intercept includes $t_{K+} = 1$, indicating that the transport number may not be significantly different from unity. A membrane with a K^+ transport number of one is a membrane perfectly selective to K^+ over Cl^-. The water transference coefficient, however, indicates that for every mole of electrons passing in the external circuit, around 3–4 moles of water pass through the ion-exchange membrane. This transported water exists as a hydration shell of 3–4 water molecules surrounding K^+ that are carried along with the ion during migration.

The AEM behaviour can be described by the intercept $100t_{K+} = -0.21 \pm 0.37$ and the slope $t_w = -3.75 \pm 0.27$. As a consequence, we have $100t_{Cl-} = (100 - 100t_{K+}) = 100.21 \pm 0.36$, indicating that the AEM is perfectly selective to Cl^-. Furthermore, a transport number equal to unity means that the co-ions, Cl^- for the CEM and K^+ for the AEM, do not enter the membrane as part of the charge conduction process. The co-ions may yet enter as part of the neutral salt KCl, then as part of the process of ordinary diffusion which does not directly affect the measured electric potential.

Both Eq. (12) and (13) were used to construct separate regressions for the data shown in Fig. 2. Comparing the two regression models in a Lack-of-Fit test with a 95% confidence level, we obtain for the CEM: $F_{LOF} = 58.5 \geq 5.2 = F_{0.95,4,5}$ for Eq. (13), and $F_{LOF} = 0.4 \leq 5.4 = F_{0.95,3,5}$ for Eq. (12). For the AEM we obtain $F_{LOF} = 180 \geq 5.2 = F_{0.95,4,5}$ for Eq. (13), and $F_{LOF} = 0.5 \leq 5.4 = F_{0.95,3,5}$ for Eq. (12). The test indicates that the model that neglects the influence of water co-transport, Eq. (13), has statistically significant trends in the data that have not been modelled. For the regression model where water co-transport is included, all significant trends in the data appear to have been modelled. Therefore, the water co-transport has a statistically significant effect on the electric potential difference across these two ion-exchange membranes.

Since cations migrate to the cathode, while anions migrate to the anode, the regression slopes of the CEM and AEM have different signs. The emergence of the sign disparity is also seen by Eq. (7) for the water transference coefficient, where we have the cross-coefficient conductivity of the cations and water minus that of the anions and water. Overall, the co-transport of water is detrimental to the open circuit potential across the ion-exchange membrane, and subsequently for the reverse electrodialysis process, in which the electric potential across many membranes in series is used to drive current in an external circuit. In a reverse electrodialysis cell, the unit cell is the smallest repeating element and consists of one CEM, one AEM and two different electrolyte compartments. With Ag/AgCl electrodes and no concentration polarisation in the bulk solutions, the electric potential difference across the unit cell is [39]:

$$\begin{aligned} -F\Delta\phi_{unit} &= (t_{K+}^{CEM} - t_{K+}^{AEM})\Delta\mu_s + (t_w^{CEM} - t_w^{AEM})\Delta\mu_w + F\frac{j}{\kappa} \\ &= (\alpha^{CEM} - \alpha^{AEM})\Delta\mu_s + F\frac{j}{\kappa} \end{aligned} \quad (15)$$

where superscripts indicate to which membrane the transport numbers and coefficients belong. The chemical potential gradients across the membrane, $\Delta\mu_s$ and $\Delta\mu_w$, have opposite signs in systems using solutions of only water and KCl. Therefore, the left hand side of Eq. (15) is positive, while the first and second terms of the right hand side are positive and negative, respectively. Other researchers have also pointed out the detrimental effect of water transport for reverse electrodialysis systems [22,39,40]. It is important to highlight that the t_w^{AEM} in Eq. (15) is negative, because cations and anions carry water in opposite directions. In the reverse electrodialysis case of a unit cell with KCl and Selemion CMVN and AMVN membranes arranged in series, we observe that approximately 8 water molecules transfer from the concentrate to the dilute compartment for every mole of electrons passing through the outer circuit.

The implications for electrodialysis, for instance for desalination purposes, are also interesting. In this process, in order to drive ions from the dilute to the concentrate compartment, the applied electric potential across the cell must exceed the electric potential that arises due to the concentration gradients (the open circuit potential). Any reduction of the open circuit potential therefore decreases the required applied electric potential for the same current density result, meaning that the water co-transport has a positive effect on electrodialysis. This may be understood by the chemical potential gradient (or simply the molarity) of water, which is positive from the dilute to the concentrate compartment. Since there is a driving force for water transport into the concentrate compartment, the hydration shell around the migrating ions may reduce the work required to force ions from the dilute to the concentrate compartment. The co-transport of water may, however, put an upper limit on the concentration obtainable for the brine solution in electrodialysis.

The transference numbers are weak functions of temperature, pressure and concentration (in a binary salt/water mixture, but in the case of multiple salts they are strong functions of composition). They are therefore indirectly related to the current density, as the passing of current may change the concentration profiles in the cell. However, in the present study we find that the assumption of constant transference numbers in the ion-exchange membranes results in all statistically significant trends modelled. It should be noted that this finding may not hold true for all salts and membranes, particularly when the system contains three or more components [41,42].

Co-transport of water in ion-exchange membranes also has implications for the membrane selectivity when there are multiple ionic species present. The aqueous ions present in the system carry hydration shells of different sizes, even inside the ion-exchange membrane phase. For instance, the water transference coefficient of a Nafion 115 cation-exchange membrane in contact with either HCl, KCl or $MgCl_2$ was determined by Okada et al. as ≈2.6, ≈5 and ≈15, respectively [13]. Water transference coefficients are obtained on a single charge basis, therefore the charge of Mg^{2+} means that each ion carries $z_{Mg^{2+}}t_w = 30$ water molecules through the Nafion 115 membrane phase. Hydrophobic membrane structures may then have a greater repelling effect on Mg^{2+} than on K^+ or H^+. Tekinalp et al. used this idea to produce AEMs that were more selective to F− and Cl^- than $SO_4{}^{2-}$ [12].

5.2. Measurements with junction electrodes

Reference electrodes with filling solutions, separated from the test solution by a liquid junction diaphragm, are commonly used in electrochemistry. The calculated permselectivities of Selemion CMVN and AMVN membranes measured with two such reference electrodes are shown in Fig. 3, where the sign of the measurement is unaltered. The measured electric potential for this cell, as seen in Appendix A, and therefore also the permselectivity, is significantly different from the first cell. With ordinary least square regression using Eq. (12), we obtain for the CEM a K^+ transport number of $100t_{K+} = 47.64 \pm 0.55$ and a water transference coefficient of $t_w = 1.95 \pm 0.40$. For the AEM,

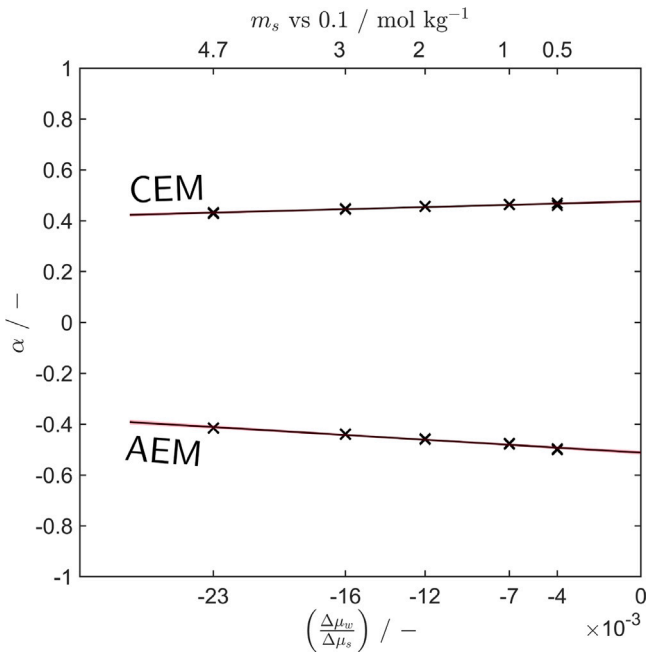

Fig. 3. Permselectivity, α, as function of the ratio of chemical potential gradients of water and salt, $\Delta\mu_w/\Delta\mu_s$, in a cell with commercial reference electrodes filled with saturated KCl. One compartment contained 0.1 mol kg^{-1} of KCl, and the top axis shows the molality of the other compartment. Measurements for the cation and anion-exchange membranes (CEM and AEM respectively) are shown as crosses, ordinary least squares regressions are shown as solid lines, and the 95% confidence interval of the regression is illustrated by the red filling. The measured cell voltage sign (and therefore permselectivity) is unaltered. (For interpretation of the references to colour in this figure legend, the reader is referred to the web version of this article.)

we obtain a K^+ transport number of $100t_{K+} = -51.20 \pm 0.81$ and a water transference coefficient of $t_w = -4.40 \pm 0.58$. The difference in permselectivities from Figs. 2 to 3 for both the CEM and the AEM is a negative shift of around $\Delta\alpha \approx -0.5$.

The voltage contribution from a single electrode junction has been measured using the scheme denoted by Cell 3, consisting of a single commercial reference electrode filled with saturated KCl measured against a Ag/AgCl rod electrode in various KCl and water solutions. The results are shown in Figs. 4–5 for each of the two junction reference electrodes used, with regressions constructed using results from the measurements at and above 0.1 mol kg^{-1}. We find that for measurements at and above 0.1 mol kg^{-1}, the data trend can be explained using Eq. (13) without water co-transport. At a 95% confidence level we obtain for Electrode 1 (Fig. 4): $F_{\mathrm{LOF}} = 4.7 \leq 5.2 = F_{0.95,4,5}$ for Eq. (13), and $F_{\mathrm{LOF}} = 2.4 \leq 5.4 = F_{0.95,3,5}$ for Eq. (12). For Electrode 2 (Fig. 5) we obtain: $F_{\mathrm{LOF}} = 4.2 \leq 5.2 = F_{0.95,4,5}$ for Eq. (13), and $F_{\mathrm{LOF}} = 0.8 \leq 5.4 = F_{0.95,3,5}$ for Eq. (12). Both models appear to have captured all trends in the data, we therefore favour the simplest model where water co-transport is neglected. The regression yields $100t_{K+} = 48.59 \pm 0.58$ for Electrode 1 shown in Fig. 4, and $100t_{K+} = 49.57 \pm 0.95$ for Electrode 2 shown in Fig. 5. The transport numbers of K^+ in the bulk of KCl/water solutions have been measured by MacInnes and Dole using the moving boundary method [29]. They reported transport numbers around $100t_{K+} = 48.98$ to 48.57 in the concentration range of 0.01 to 3.0 mol dm^{-3}. These results indicate that the porous junctions in these commercial reference electrodes have practically the same transport characteristics as bulk KCl dissolved in water in the range 0.1 mol kg^{-1} to saturation.

Below 0.1 mol kg^{-1}, the recorded cell voltage deviated from the expected values, and the deviation was unequal for the two junction reference electrodes. Furthermore, the exact magnitude of the deviation was not reproducible, but varied in each repetition of the measurement.

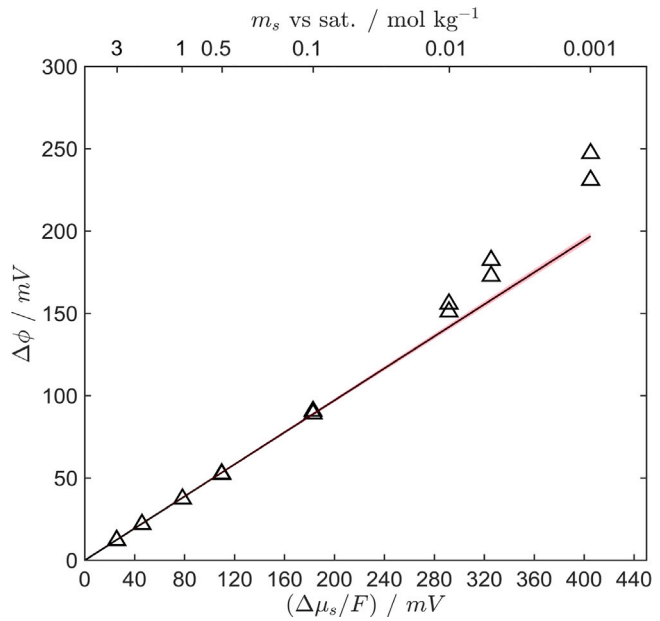

Fig. 4. Measured electric potential, $\Delta\phi$, as function of the chemical potential gradient of salt, $\Delta\mu_s/F$, in the cell with the commercial reference electrode number 1 against an Ag rod electrode. One compartment contained saturated KCl, and the top axis shows the molality of the other compartment. Measurements are shown as triangles, ordinary least squares regressions are shown as solid lines, and the 95% confidence interval of the regression is illustrated by the red filling. (For interpretation of the references to colour in this figure legend, the reader is referred to the web version of this article.)

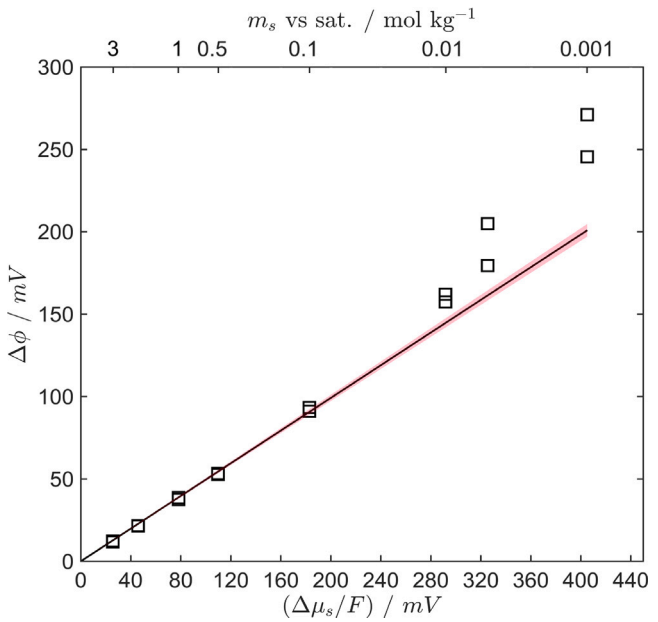

Fig. 5. Measured electric potential, $\Delta\phi$, as function of the chemical potential gradient of salt, $\Delta\mu_s/F$, in the cell with the commercial reference electrode number 2 against an Ag rod electrode. One compartment contained saturated KCl, and the top axis shows the molality of the other compartment. Measurements are shown as squares, ordinary least squares regressions are shown as solid lines, and the 95% confidence interval of the regression is illustrated by the red filling. (For interpretation of the references to colour in this figure legend, the reader is referred to the web version of this article.)

These experiments were continued for up to four hours, at which point the cell voltage remained stable. By plotting the results as α versus $\Delta\mu_w/\Delta\mu_s$ we find that the deviations are consistent with increased K^+ transport numbers and water transference coefficients from around $t_{K+} \approx 0.5$ and $t_w \approx 0$ to $t_{K+} \approx 0.8$ and $t_w \approx 18$. Stated differently, the ceramic diaphragm junction appeared to become more selective to K^+ when in contact with very dilute KCl solutions. We suspect that if the interior of this porous junction favours transport of K^+ at dilute concentrations, the poor reproducibility in this range may have been due to differently shaped concentration gradients developing across the porous junction in each repeated measurement. Both very large concentration gradients and the same very dilute concentrations were also tested in the Cell 1 configuration to gauge whether the same anomalous behaviour occurs for the membranes. However, the ion-exchange membranes remained selective according to the trend shown in Fig. 2.

The electric potential contribution of two junction reference electrodes in series may also be accessed by taking the measured voltage of Cell 2 minus the voltage of Cell 1 for the same conditions across the membrane. The same quantity is accessible by subtracting voltage values of junction electrode number 1 (Fig. 4) from electrode number 2 (Fig. 5). Values are provided in Table 1. There is good agreement between values derived from the three methods. An average of all three derivations is well explained by Eq. (13) and $100t_{K+} = 49.43 \pm 0.78$, further supporting the argument that the electrode junctions behave as bulk KCl at concentrations above 0.1 mol kg^{-1}. This contribution to the measured voltage of the concentration cell means that the membrane potential is more directly accessed by using bare Ag/AgCl electrodes in the case of a Cl^- containing electrolyte.

Table 1
The electric potential contribution from the two junction electrodes in Cell 2, one of which immersed in 0.1 mol kg^{-1} and one in m_s mol kg^{-1} KCl, derived from measurements of Cell 1 and Cell 2 with a CEM, an AEM, and from the Cell 3 junction measurements. The calculated ideal electric potential difference, $\Delta\mu_s/F$, is included for reference.

m_s	0.1 vs.				
	4.7	3	2	1	0.5
$\Delta\phi$ (CEM)	90.73	77.79	68.59	52.40	37.58
$\Delta\phi$ (AEM)	87.49	77.43	67.84	52.76	37.80
$\Delta\phi$ (junc.)	89.06	77.02	67.31	51.80	36.39
$\Delta\mu_s/F$	182.18	156.89	136.75	104.42	73.04

6. Conclusions

The concept of permselectivity, here defined as the measured electric potential divided by the ideal potential, has been used to characterise the selectivity of Selemion CMVN and AMVN cation and anion-exchange membranes in solutions of KCl and water. We have analysed the measurements using the framework of non-equilibrium thermodynamics, where the permselectivity can be derived as a function of chemical potential gradients across the membrane and the membrane transference coefficients of salt and water. The choice of Cl^- reversible electrodes defines the measurable electric potential in the system, giving $t_s = t_{K+}$ for the investigated system. Electrodes with and without liquid junctions and filling solutions were used to measure the electric potential across ion-exchange membranes, and additional experiments were conducted to isolate the contribution from the junctions.

The measurable electric potential difference across only the membrane was more easily determined using bare Ag/AgCl electrodes compared to the use of electrodes with liquid junctions and filling solutions. The transport number of K^+ in the Selemion CMVN cation-exchange membrane was determined to be $100t_{K+} = 99.59 \pm 0.56$ and the water transference coefficient to be $t_w = 3.69 \pm 0.40$. For the Selemion AMVN anion-exchange membrane, we obtained $100t_{K+} = -0.21 \pm 0.37$ and $t_w = -3.75 \pm 0.27$, and as a consequence $100t_{Cl-} = (100 - 100t_{K+}) = 100.21 \pm 0.37$. Therefore, the membranes are assessed to be perfectly selective to their corresponding ionic species in solutions of KCl. However, the water co-transport was found to be statistically significant, and each ion passing the membrane carried 3–4 molecules of water. This electroosmotic transport has a detrimental effect on the permselectivity that increases with the magnitude of the chemical potential gradients across

the membrane. Consequences of this effect depend on the process, as it reduces the available work from the controlled salt mixing process in reverse electrodialysis, but it also reduces the required work to reverse the mixing process in an electrodialysis process.

We find that transport through the electrode liquid junctions is well described by the transport properties of bulk KCl when the junction electrode is immersed in solutions with concentrations above 0.1 mol kg^{-1}, and with negligible water co-transport. Above 0.1 mol kg^{-1}, we find $100t_{K+} = 49.43 \pm 0.78$. When the electrode was immersed in more dilute concentrations of KCl, we observed an increase in the transport number of K^+ and the water transference coefficient. This suggests that these particular ceramic porous junctions become more selective when immersed in dilute KCl. As a consequence, electrodes without liquid junctions should be used to measure ion-exchange membrane properties, if it is possible for the investigated electrolyte system. Some additional work is required to replenish the electrodes to keep the bias potential low and stable, but one avoids the need to correct for a potentially large junction potential which may or may not have the same transport characteristics as the bulk electrolyte.

CRediT authorship contribution statement

Simon B.B. Solberg: Conceptualization, Methodology, Formal analysis, Investigation, Data curation, Writing – original draft, Visualization, Project administration. **Pauline Zimmermann:** Conceptualization, Writing – review & editing. **Øivind Wilhelmsen:** Writing – review & editing, Supervision, Project administration, Funding acquisition. **Robert Bock:** Writing – review & editing, Supervision, Project administration. **Odne S. Burheim:** Resources, Writing – review & editing, Supervision, Project administration, Funding acquisition.

Data availability

Data will be made available on request.

Acknowledgements

The authors are grateful for support and funding from the ENERSENSE research initiative (Grant Number 68024013) at the Norwegian University of Science and Technology, and the Department of Energy and Process Engineering through the project number 81772020. Ø.W. acknowledges funding from the Research Council of Norway (RCN), the Center of Excellence Funding Scheme, Project No. 262644, PoreLab. The authors also wish to thank Professor Magne Hillestad for an interesting and helpful discussion on regression statistics.

Declaration of competing interest

The authors declare that they have no known competing financial interests or personal relationships that could have appeared to influence the work reported in this paper.

Appendix A. Measured cell potentials

The measured cell potentials, with electrode bias subtracted, for the cells with Ag/AgCl rods (Cell 1) and Ag/AgCl junction electrodes (Cell 2) and Selemion CMVN and AMVN membranes are shown in Table A.2. Measured cell potentials between a single junction electrode with saturated KCl filling and a Ag/AgCl rod electrode in various KCl/water solutions (Cell 3) are shown in Table A.3.

Appendix B. Thermodynamic data

Thermodynamic data for the binary mixture of KCl and water are necessary for the calculation of chemical potentials of the components. The departure from ideal behaviour for the electrolyte mixture is described by either the salt activity coefficient, $\gamma_{\pm}$, or the osmotic coefficient, φ. If one is known then the other coefficient follows from the Gibbs–Duhem equation. Both coefficients have been extensively researched for KCl/water systems. Activity coefficients as functions of KCl molality, m_s, at standard conditions have been reviewed and summarised by Hamer and Wu [31]. These data points are shown in Fig. B.6, where some outliers and re-calculations of the same measurement data were excluded.

The Pitzer equations constitute a useful model for the behaviour of the salt activity as a function of composition, temperature and pressure [43]. For a binary monovalent salt (for which the ionic strength is equal to the molality), these equations may be expressed as a multiple linear regression of the form:

$$\ln \gamma_{\pm} + A_{\varphi}\left[\frac{\sqrt{m_s}}{1+b\sqrt{m_s}} + \frac{a}{b}\ln\left(1+b\sqrt{m_s}\right)\right] = 2\beta_1 m_s + \beta_2 \frac{f(m_s)}{a} + \frac{3}{2}\beta_3 m_s^2 \tag{B.1}$$

Table A.2
Measured cell potentials, with electrode bias subtracted, of the cells with bare Ag/AgCl rods (Cell 1) denoted by "R" with the run number specified in parenthesis, and of cells with Ag/AgCl junction electrodes (Cell 2) denoted by "J". Measurements are given with 95% confidence intervals, and were conducted with 0.1 and m_s mol kg^{-1} KCl on either side of the membrane.

m_s	CEM R(1)	CEM R(2)	AEM R(1)	AEM R(2)	CEM J(1)	CEM J(2)	AEM J(1)	AEM J(2)
4.8	165.01 (± 1.65)	166.35 (± 1.78)	15.70 (± 2.1)	14.89 (± 2.26)	78.62 (± 1.73)	77.77 (± 1.79)	−75.37 (± 0.86)	−75.49 (± 0.87)
3	147.12 (± 1.41)	148.16 (± 1.38)	8.36 (± 1.13)	9.02 (± 1.05)	69.94 (± 1.15)	70.47 (± 1.71)	−69.21 (± 0.87)	−68.99 (± 0.88)
2	129.88 (± 1.43)	130.85 (± 1.33)	5.72 (± 1.08)	5.89 (± 1.06)	62.63 (± 1.26)	62.43 (± 1.37)	−62.54 (± 0.88)	−63.02 (± 0.94)
1	101.14 (± 1.23)	101.50 (± 1.22)	2.32 (± 1.04)	2.74 (± 1.01)	48.69 (± 1.22)	48.43 (± 1.33)	−49.68 (± 1.03)	−50.06 (± 0.90)
0.5	71.71 (± 1.15)	71.87 (± 1.19)	0.92 (± 1.01)	1.21 (± 1.01)	33.67 (± 1.07)	34.31 (± 1.07)	−36.34 (± 0.96)	−36.68 (± 0.93)

Table A.3
Measured cell potentials, with electrode bias subtracted, of the cell with one bare Ag/AgCl rod and one junction electrode (Cell 3) for each of the two junction electrodes EL#1 and EL#2, with the run number specified in parenthesis. Measurements are given with 95% confidence intervals, and were conducted with a saturated KCl filling in the junction electrode and m_s mol kg^{-1} KCl in the external test solution.

m_s	EL#1 (1)	EL#1 (2)	EL#2 (1)	EL#2 (2)
3	12.04 (± 1.04)	12.26 (± 1.02)	12.29 (± 1.03)	11.73 (± 1.03)
2	21.75 (± 1.07)	21.90 (± 1.08)	21.68 (± 1.15)	21.29 (± 1.33)
1	37.26 (± 1.09)	37.33 (± 1.08)	37.48 (± 1.09)	38.70 (± 1.18)
0.5	52.67 (± 1.14)	52.21 (± 1.81)	52.70 (± 1.21)	53.33 (± 1.11)
0.1	89.06 (± 1.18)	90.60 (± 1.20)	90.98 (± 1.37)	93.32 (± 1.19)
0.01	155.81 (± 1.66)	151.01 (± 2.53)	162.01 (± 1.43)	157.35 (± 1.58)
0.005	182.33 (± 1.93)	172.69 (± 2.17)	204.87 (± 3.03)	179.33 (± 1.45)
0.001	247.15 (± 2.79)	230.97 (± 2.03)	271.08 (± 2.52)	245.62 (± 1.53)

Table B.4
Fitted Pitzer parameters for the activity and osmotic coefficient regressions of KCl at various temperatures [31–36]. Parameters are given with 95% confidence intervals.

	$\beta_1 \times 100$	$\beta_2 \times 100$	$\beta_3 \times 100$
0 ° C	2.21 (± 0.49)	20.19 (± 1.79)	0.45 (± 0.15)
10 ° C	3.56 (± 0.23)	20.79 (± 0.84)	0.15 (± 0.07)
18 ° C	3.97 (± 1.30)	21.77 (± 2.68)	0.15 (± 1.01)
20 ° C	4.53 (± 0.23)	21.73 (± 0.95)	−0.04 (± 0.06)
25 ° C	4.63 (± 0.25)	22.84 (± 1.03)	−0.04 (± 0.06)
40 ° C	5.42 (± 0.34)	23.96 (± 1.37)	−0.14 (± 0.09)
50 ° C	5.68 (± 0.90)	23.75 (± 3.43)	−0.09 (± 0.26)
60 ° C	6.08 (± 0.18)	26.08 (± 0.73)	−0.20 (± 0.05)
70 ° C	6.37 (± 0.18)	26.61 (± 0.70)	−0.23 (± 0.05)
80 ° C	6.65 (± 0.23)	27.45 (± 0.89)	−0.29 (± 0.06)

Table B.5
Fitted parameters for the temperature variation of the Pitzer regressions for KCl [31–36]. Parameters are given with 95% confidence intervals.

	χ_1	χ_2	$\chi_3 \times 100$
β_1	1.09 (± 0.49)	−185.94 (± 75.51)	−0.14 (± 0.08)
β_2	0.52 (± 0.04)	−89.35 (± 13.43)	0
β_3	−0.22 (± 0.19)	38.43 (± 29.76)	0.03 (± 0.03)

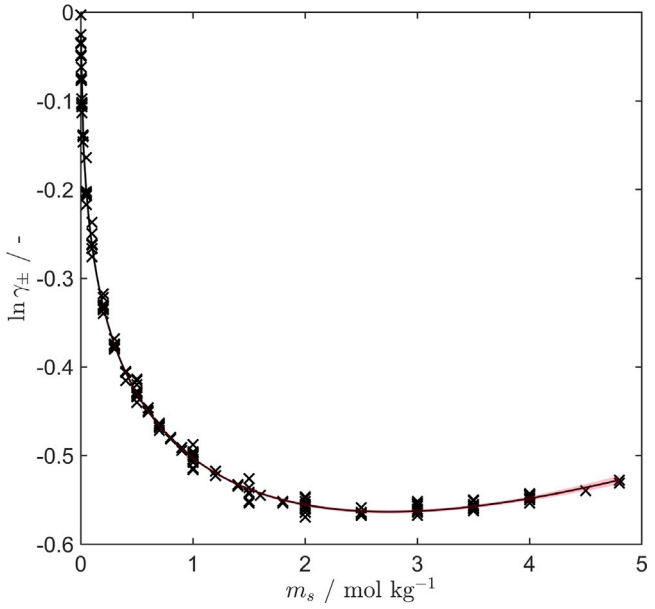

Fig. B.6. Activity coefficient of KCl, $\gamma_{\pm}$, as function of the salt molality, m_s, at room temperature, $T = 298.15$ K, and atmospheric pressure. Measurement points are given by crosses, and the Pitzer regression is shown as a solid line. The 95% confidence interval for the regression is shown in red. (For interpretation of the references to colour in this figure legend, the reader is referred to the web version of this article.)

where A_φ is the Debye–Hückel limiting slope as evaluated by Clarke and Glew [44], $a = 2$ kg$^{1/2}$ mol$^{-1/2}$ and $b = 1.2$ kg$^{1/2}$ mol$^{-1/2}$ are constants for all monovalent salts, β_i are regression coefficients, and the function $f(m_s) = 1 - \exp(-a\sqrt{m_s})(1 + a\sqrt{m_s} - am_s)$. The osmotic coefficient is given in terms of the same regression coefficients:

$$\varphi - 1 + A_\varphi \left(\frac{\sqrt{m_s}}{1 + b\sqrt{m_s}} \right) = \beta_1 m_s + \beta_2 \exp(-a\sqrt{m_s}) + \beta_3 m_s^2 \tag{B.2}$$

The variation of the KCl activity coefficient with temperature has been measured by multiple authors in the range of 0 °C to 80 °C [32–36]. By fitting regression coefficients for the activity coefficients at each temperature, as shown in Table B.4, it is possible to estimate the dependence on temperature of the coefficients. Some confidence intervals for β_3 contained zero, so that a marginally better model for these particular data sets may be obtained by excluding this parameter.

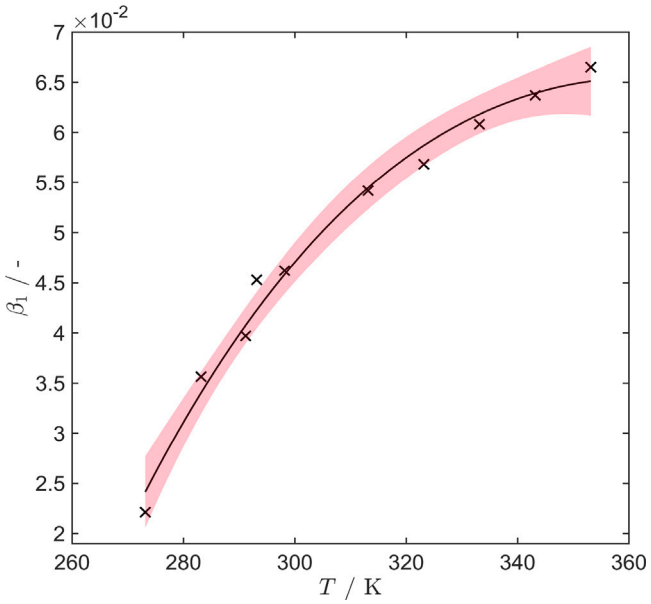

Fig. B.7. Variation of the first Pitzer regression coefficient with temperature. Regression coefficients at each temperature is given by crosses, the regression 95% confidence interval is shown in red, and the solid line is given by the regression $\beta_1 = \chi_1 + \frac{\chi_2}{T} + \chi_3 T$. (For interpretation of the references to colour in this figure legend, the reader is referred to the web version of this article.)

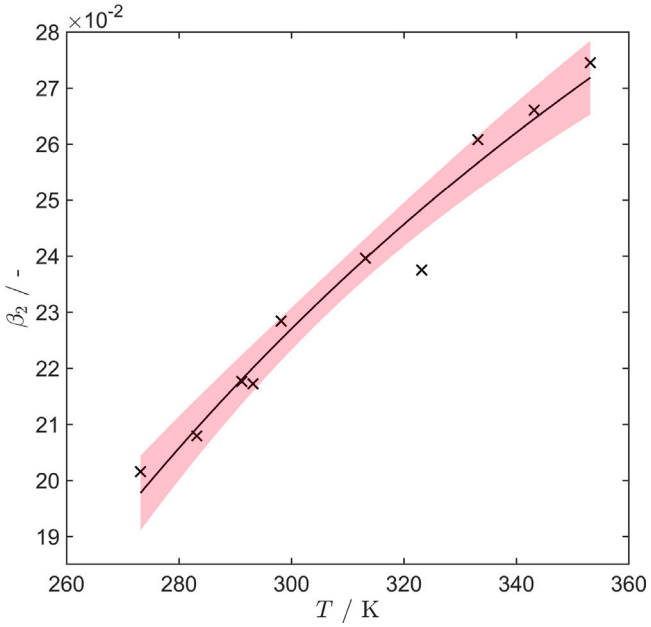

Fig. B.8. Variation of the second Pitzer regression coefficient with temperature. Regression coefficients at each temperature is given by crosses, the regression 95% confidence interval is shown in red, and the solid line is given by the regression $\beta_2 = \chi_1 + \frac{\chi_2}{T}$. (For interpretation of the references to colour in this figure legend, the reader is referred to the web version of this article.)

Despite of this, it has been kept for simplicity's sake. The regression coefficients are shown as functions of temperature in Figs. B.7–B.9. For the coefficients β_1 and β_3, a three parameter model describes the trend well:

$$\beta_{i\neq 2} = \chi_1 + \frac{\chi_2}{T} + \chi_3 T \tag{B.3}$$

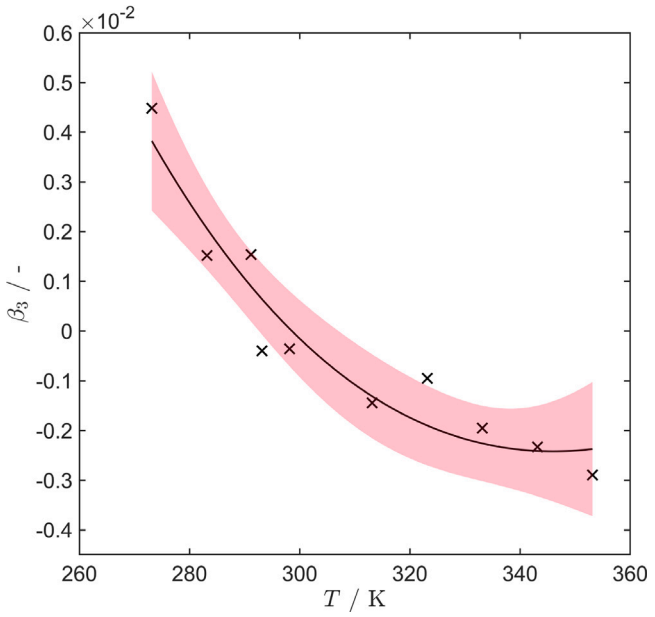

Fig. B.9. Variation of the third Pitzer regression coefficient with temperature. Regression coefficients at each temperature is given by crosses, the regression 95% confidence interval is shown in red, and the solid line is given by the regression $\beta_3 = \chi_1 + \frac{\chi_2}{T} + \chi_3 T$. (For interpretation of the references to colour in this figure legend, the reader is referred to the web version of this article.)

while the coefficient β_2 was best described by:

$$\beta_2 = \chi_1 + \frac{\chi_2}{T} \tag{B.4}$$

The models were chosen such that the 95% confidence interval of each parameter did not include zero. These regression coefficients are summarised in Table B.5.

References

[1] R. Nagarale, G. Gohil, V.K. Shahi, Recent developments on ion-exchange membranes and electro-membrane processes, Adv. Colloid Interface Sci. (ISSN: 0001-8686) 119 (2) (2006) 97–130, http://dx.doi.org/10.1016/j.cis.2005.09.005, URL https://www.sciencedirect.com/science/article/pii/S0001868605001107.

[2] S. Al-Amshawee, M.Y.B.M. Yunus, A.A.M. Azoddein, D.G. Hassell, I.H. Dakhil, H.A. Hasan, Electrodialysis desalination for water and wastewater: A review, Chem. Eng. J. (ISSN: 1385-8947) 380 (2020) 122231, http://dx.doi.org/10.1016/j.cej.2019.122231, URL https://www.sciencedirect.com/science/article/pii/S1385894719316250.

[3] T. Xu, Ion exchange membranes: State of their development and perspective, J. Membr. Sci. (ISSN: 0376-7388) 263 (1) (2005) 1–29, http://dx.doi.org/10.1016/j.memsci.2005.05.002, URL https://www.sciencedirect.com/science/article/pii/S0376738805003571.

[4] Y. Mei, C.Y. Tang, Recent developments and future perspectives of reverse electrodialysis technology: A review, Desalination (ISSN: 0011-9164) 425 (2018) 156–174, http://dx.doi.org/10.1016/j.desal.2017.10.021, URL https://www.sciencedirect.com/science/article/pii/S001191641731977X.

[5] M.C. Hatzell, I. Ivanov, R. D. Cusick, X. Zhu, B.E. Logan, Comparison of hydrogen production and electrical power generation for energy capture in closed-loop ammonium bicarbonate reverse electrodialysis systems, Phys. Chem. Chem. Phys. 16 (2014) 1632–1638, http://dx.doi.org/10.1039/C3CP54351J, URL http://dx.doi.org/10.1039/C3CP54351J.

[6] S.B.B. Solberg, P. Zimmermann, Ø. Wilhelmsen, J.J. Lamb, R. Bock, O.S. Burheim, Heat to hydrogen by reverse electrodialysis; using a non-equilibrium thermodynamics model to evaluate hydrogen production concepts utilising waste heat, Energies (ISSN: 1996-1073) 15 (16) (2022) http://dx.doi.org/10.3390/en15166011, URL https://www.mdpi.com/1996-1073/15/16/6011.

[7] P. Zimmermann, S.B.B. Solberg, Ö. Tekinalp, J.J. Lamb, Ø. Wilhelmsen, L. Deng, O.S. Burheim, Heat to hydrogen by red; reviewing membranes and salts for the RED heat engine concept, Membranes (ISSN: 2077-0375) 12 (1) (2022) http://dx.doi.org/10.3390/membranes12010048, URL https://www.mdpi.com/2077-0375/12/1/48.

[8] A. Ranade, K. Singh, A. Tamburini, G. Micale, D.A. Vermaas, Feasibility of producing electricity, hydrogen, and chlorine via reverse electrodialysis, Environ. Sci. Technol. 56 (22) (2022) 16062–16072, http://dx.doi.org/10.1021/acs.est.2c03407.

[9] M. Mulder, J. Mulder, Basic Principles of Membrane Technology, Springer Science & Business Media, 1996.

[10] T. Luo, S. Abdu, M. Wessling, Selectivity of ion exchange membranes: A review, J. Membr. Sci. (ISSN: 0376-7388) 555 (2018) 429–454, http://dx.doi.org/10.1016/j.memsci.2018.03.051, URL https://www.sciencedirect.com/science/article/pii/S0376738817335779.

[11] S. Kjelstrup, D. Bedeaux, Non-Equilibrium Thermodynamics of Heterogeneous Systems, World Scientific, Singapore, 2008.

[12] Ö. Tekinalp, P. Zimmermann, O.S. Burheim, L. Deng, Designing monovalent selective anion exchange membranes for the simultaneous separation of chloride and fluoride from sulfate in an equimolar ternary mixture, J. Membr. Sci. (ISSN: 0376-7388) 666 (2023) 121148, http://dx.doi.org/10.1016/j.memsci.2022.121148, URL https://www.sciencedirect.com/science/article/pii/S0376738822008936.

[13] T. Okada, N. Nakamura, M. Yuasa, I. Sekine, Ion and water transport characteristics in membranes for polymer electrolyte fuel cells containing H+ and Ca^{2}+ cations, J. Electrochem. Soc. 144 (8) (1997) 2744, http://dx.doi.org/10.1149/1.1837890.

[14] T. Okada, S. Møller-Holst, O. Gorseth, S. Kjelstrup, Transport and equilibrium properties of Nafion® membranes with H+ and Na+ ions, J. Electroanal. Soc. (ISSN: 1572-6657) 442 (1) (1998) 137–145, http://dx.doi.org/10.1016/S0022-0728(97)00499-3, URL https://www.sciencedirect.com/science/article/pii/S0022072897004993.

[15] T. Okada, H. Satou, M. Okuno, M. Yuasa, Ion and water transport characteristics of perfluorosulfonated ionomer membranes with H+ and alkali metal cations, J. Phys. Chem. B 106 (6) (2002) 1267–1273, http://dx.doi.org/10.1021/jp013195l.

[16] H.R. Zelsmann, M. Pineri, M. Thomas, M. Escoubes, Water self-diffusion coefficient determination in an ion exchange membrane by optical measurement, J. Appl. Polym. Sci. 41 (7–8) (1990) 1673–1684, http://dx.doi.org/10.1002/app.1990.070410726, URL https://onlinelibrary.wiley.com/doi/abs/10.1002/app.1990.070410726.

[17] T.A.J. Zawodzinski, M. Neeman, L.O. Sillerud, S. Gottesfeld, Determination of water diffusion coefficients in perfluorosulfonate ionomeric membranes, J. Phys. Chem. 95 (15) (1991) 6040–6044, http://dx.doi.org/10.1021/j100168a060.

[18] T.A. Zawodzinski, C. Derouin, S. Radzinski, R.J. Sherman, V.T. Smith, T.E. Springer, S. Gottesfeld, Water uptake by and transport through Nafion® 117 membranes, J. Electrochem. Soc. 140 (4) (1993) 1041, http://dx.doi.org/10.1149/1.2056194.

[19] T.F. Fuller, J. Newman, Experimental determination of the transport number of water in Nafion 117 membrane, J. Electrochem. Soc. 139 (5) (1992) 1332, http://dx.doi.org/10.1149/1.2069407.

[20] G. Xie, T. Okada, Characteristics of water transport in relation to microscopic structure in nafion membranes, J. Chem. Soc. Faraday Trans. 92 (4) (1996) 663–669.

[21] G. Xie, T. Okada, Pumping effects in water movement accompanying cation transport across nafion 117 membranes, Electrochim. Acta (ISSN: 0013-4686) 41 (9) (1996) 1569–1571, http://dx.doi.org/10.1016/0013-4686(95)00391-6, URL https://www.sciencedirect.com/science/article/pii/0013468695003916.

[22] A. Zlotorowicz, R. Strand, O. Burheim, Ø. Wilhelmsen, S. Kjelstrup, The permselectivity and water transference number of ion exchange membranes in reverse electrodialysis, J. Membr. Sci. (ISSN: 0376-7388) 523 (2017) http://dx.doi.org/10.1016/j.memsci.2016.10.003, URL https://www.sciencedirect.com/science/article/pii/S0376738816318208.

[23] M. Ottøy, T. Førland, S.K. Ratkje, S. Møller-Holst, Membrane transference numbers from a new emf method, J. Membr. Sci. (ISSN: 0376-7388) 74 (1) (1992) 1–8, http://dx.doi.org/10.1016/0376-7388(92)87067-8, URL https://www.sciencedirect.com/science/article/pii/0376738892870678.

[24] T. Okada, S. Kjelstrup-Ratkje, S. Møller-Holst, L. Jerdal, K. Friestad, G. Xie, R. Holmen, Water and ion transport in the cation exchange membrane systems nacl-SrCl2 and KCl-SrCl2, J. Membr. Sci. (ISSN: 0376-7388) 111 (2) (1996) 159–167, http://dx.doi.org/10.1016/0376-7388(95)00184-0, URL https://www.sciencedirect.com/science/article/pii/0376738895001840.

[25] E.E. Johnsen, S.K. Ratkje, T. Førland, K.S. Førland, The liquid junction contribution to emf, Z. Phys. Chem. 168 (1) (1990) 101–114, http://dx.doi.org/10.1524/zpch.1990.168.Part_1.101.

[26] A.S. Gangrade, S. Cassegrain, P. Chandra Ghosh, S. Holdcroft, Permselectivity of ionene-based, Aemion® anion exchange membranes, J. Membr. Sci. (ISSN: 0376-7388) 641 (2022) 119917, http://dx.doi.org/10.1016/j.memsci.2021.119917, URL https://www.sciencedirect.com/science/article/pii/S0376738821008607.

[27] E.A. Guggenheim, The conceptions of electrical potential difference between two phases and the individual activities of ions, J. Phys. Chem. 33 (6) (1929) 842–849, http://dx.doi.org/10.1021/j150300a003.

[28] P.B. Taylor, Electromotive force of the cell with transference and theory of interdiffusion of electrolytes, J. Phys. Chem. 31 (10) (1927) 1478–1500, http://dx.doi.org/10.1021/j150280a002.

[29] D.A. MacInnes, M. Dole, The transference numbers of potassium chloride. new determinations by the Hittorf method and a comparison with results obtained by the moving boundary method, J. Am. Chem. Soc. 53 (4) (1931) 1357–1364, http://dx.doi.org/10.1021/ja01355a025.

[30] R. Robinson, R. Stokes, Electrolyte Solutions: Second Revised Edition, in: Dover Books on Chemistry Series, Dover Publications Incorporated, ISBN: 9780486138787, 1959.

[31] W.J. Hamer, Y.-C. Wu, Osmotic coefficients and mean activity coefficients of uni-univalent electrolytes in water at 25°C, J. Phys. Chem. Ref. Data 1 (4) (1972) 1047–1100, http://dx.doi.org/10.1063/1.3253108.

[32] H.S. Harned, M.A. Cook, The thermodynamics of aqueous potassium chloride solutions from electromotive force measurements, J. Am. Chem. Soc. 59 (7) (1937) 1290–1292, http://dx.doi.org/10.1021/ja01286a038.

[33] H.P. Snipes, C. Manly, D.D. Ensor, Heats of dilution of aqueous electrolytes. Temperature dependence, J. Chem. Eng. Data 20 (3) (1975) 287–291, http://dx.doi.org/10.1021/je60066a027.

[34] T.M. Herrington, R.J. Jackson, Osmotic coefficients of aqueous potassium chloride solutions at 50 and 70°C, J. Chem. Soc. Faraday Trans. I 69 (1973) 1635–1647, http://dx.doi.org/10.1039/F19736901635.

[35] R.P. Smith, The activity coefficient of potassium chloride in aqueous solutions at 0°C from electromotive force and freezing point data, J. Am. Chem. Soc. 55 (8) (1933) 3279–3282, http://dx.doi.org/10.1021/ja01335a038.

[36] P.B. Hostetler, A.H. Truesdell, C.L. Christ, Activity coefficients of aqueous potassium chloride measured with a potassium-sensitive glass electrode, Science 155 (3769) (1967) 1537–1539, http://dx.doi.org/10.1126/science.155.3769.1537, URL https://www.science.org/doi/abs/10.1126/science.155.3769.1537.

[37] G. Box, J. Hunter, W. Hunter, Statistics for Experimenters: Design, Innovation, and Discovery, in: Wiley Series in Probability and Statistics, Wiley, ISBN: 9780471718130, 2005, URL https://books.google.no/books?id=oYUpAQAAMAAJ.

[38] S. Ito, H. Hachiya, K. Baba, Y. Asano, H. Wada, Improvement of the silver/silver chloride reference electrode and its application to pH measurement, Talanta (ISSN: 0039-9140) 42 (11) (1995) 1685–1690, http://dx.doi.org/10.1016/0039-9140(95)01628-7, URL https://www.sciencedirect.com/science/article/pii/0039914095016287.

[39] K.R. Kristiansen, V.M. Barragán, S. Kjelstrup, Thermoelectric power of ion exchange membrane cells relevant to reverse electrodialysis plants, Phys. Rev. A 11 (2019) 044037, http://dx.doi.org/10.1103/PhysRevApplied.11.044037, URL https://link.aps.org/doi/10.1103/PhysRevApplied.11.044037.

[40] F. Malatesta, G. Carrara, Activity coefficients of electrolytes from the E.M.F. of liquid membrane cells. I. The method—Test measurements on KCl, J. Solut. Chem. 21 (1992) 1251–1270, http://dx.doi.org/10.1007/BF00667221.

[41] H. Schönert, Transference numbers in the H2O+NaCl+MgCl2 system at T=298.15 K, determined in a five-compartment Hittorf cell, J. Solut. Chem. 43 (1) (2014) 26–39, http://dx.doi.org/10.1007/s10953-012-9944-y.

[42] T. Jung, A.A. Wang, C.W. Monroe, Overpotential from cosolvent imbalance in battery electrolytes: LiPF6 in EMC:EC, ACS Omega 8 (23) (2023) 21133–21144, http://dx.doi.org/10.1021/acsomega.3c02088.

[43] P.P.S. Saluja, K.S. Pitzer, R.C. Phutela, High-temperature thermodynamic properties of several 1:1 electrolytes, Can. J. Chem. 64 (7) (1986) 1278–1285, http://dx.doi.org/10.1139/v86-220.

[44] E.C.W. Clarke, D.N. Glew, Evaluation of Debye–Hückel limiting slopes for water between 0 and 150°C, J. Chem. Soc. Faraday Trans. I 76 (1980) 1911–1916, http://dx.doi.org/10.1039/F19807601911.